Phonon frequencies of a highly strained AlN layer coherently grown on 6H-SiC (0001)

AUTHOR(S):

Kaneko, M.; Kimoto, T.; Suda, J.

CITATION:

Kaneko, M. ...[et al]. Phonon frequencies of a highly strained AlN layer coherently grown on 6H-SiC (0001). AIP Advances 2017, 7(1): 015105.

ISSUE DATE:

2017-01

URL:

http://hdl.handle.net/2433/218240

Phonon frequencies of a highly strained AlN layer coherently grown on 6H-SiC (0001)

M. Kaneko, T. Kimoto, and J. Suda

Citation: AIP Advances **7**, 015105 (2017); doi: 10.1063/1.4974500
View online: http://dx.doi.org/10.1063/1.4974500
View Table of Contents: http://aip.scitation.org/toc/adv/7/1
Published by the American Institute of Physics

AIP ADVANCES 7, 015105 (2017)

Phonon frequencies of a highly strained AlN layer coherently grown on 6H-SiC (0001)

M. Kaneko,[a] T. Kimoto, and J. Suda
Department of Electronic Science and Engineering, Kyoto University, Kyoto 615-8510, Japan

(Received 6 December 2016; accepted 9 January 2017; published online 18 January 2017)

Phonon frequencies of a high-quality AlN layer coherently grown on a 6H-SiC (0001) substrate are investigated by Raman scattering. Owing to the largest strain in our coherent AlN layer among heteroepitaxially grown AlN layers ever reported, phonon frequencies of the E_2 (low), E_2 (high), and A_1 (LO) modes are considerably shifted to 244.5 (−3.3, compared with bulk AlN), 672.1 (+16.3), and 899 (+11) cm^{-1}, respectively. Full widths at half maximum of the phonon modes in the coherent AlN are almost equal to those of high-quality bulk AlN, clearly indicating its high crystalline quality and uniform strain. We discuss accuracy of phonon deformation potentials reported by several other groups thorough comparing our experimental results. [http://dx.doi.org/10.1063/1.4974500]

Raman scattering is a powerful tool to investigate strain states since Raman spectra can easily be obtained without special sample preparation.[1,2] By focusing incident light through optical lenses, high spatial resolution (~1 μm) can also be achieved.[3,4] To obtain strain states from Raman spectra, phonon deformation potentials (PDPs) are needed. The PDPs of gallium nitride (GaN) are well studied by both theoretical calculations and experiments.[5–7] On the other hand, study of the PDPs of aluminum nitride (AlN) is still immature and there is a great discrepancy between reports.[8–14] As an experimental report, Yang et al.[11] obtained PDPs using several lattice-relaxed AlN heteroepitaxial layers with various residual strains. In lattice-relaxed AlN layers, however, high-density defects and strain distribution make it difficult to obtain accurate values of not only lattice constants but also phonon frequency shifts, resulting in inaccurate PDP values. Recently, Callsen et al.[14] obtained PDPs through uniaxial pressure dependence of phonon frequency shifts in hiqh-quality bulk AlN. The study gives reliable PDPs owing to both their careful experiments and quality of the bulk AlN. However, derivation of the PDPs needs elastic stiffness constants (C_{ij}) of AlN, the values of which also diverse between reports.[15–17] Therefore, there is still room to discuss accuracy of the PDPs in AlN.

In previous studies, we have focused on AlN growth on SiC substrates by rf-plasma-assisted molecular beam epitaxy (rf-MBE). By controlling the initial growth, we have realized high-quality growth of wurtzite AlN on 6H-SiC (0001), which is coherently grown up to 700 nm.[18] The high-quality AlN shows uniform strain, resulting in very narrow high-resolution x-ray diffraction (HRXRD) ω-scan peaks and sharp free exciton emissions in low-temperature photoluminescence.[19,20] Because this coherent AlN has the largest strain among heteroepitaxially grown AlN layers ever reported, the AlN gives reliable and irreplaceable data about AlN material properties related to strain. In this study, phonon frequencies of the coherent AlN are evaluated by Raman scattering. As for a reference of strain-free AlN, high-quality bulk AlN grown by physical vapor transport (PVT) method is also measured. Due to the large strain, large frequency shifts are observed. Based on the obtained data, accuracy of the reported PDPs is discussed.

[a]Electronic mail: kaneko@semicon.kuee.kyoto-u.ac.jp.

The 300-nm-thick AlN layer was grown by rf-MBE on a 6H-SiC (0001) Si-face substrate with a miscut of 0.08°. The growth condition is found elsewhere.[19] HRXRD was used to obtain lattice constants. By 2θ- ω scans of (0004), (10$\bar{1}$5), and (20$\bar{2}$4) (high-angle reflection), a- and c-axis lattice constants were precisely determined to be 3.0815 and 5.0063 Å, respectively. The a-axis lattice constant of SiC substrate (3.0809 Å) was equal to that of the grown AlN within measurement error (± 0.0005 Å), clearly indicating its coherent growth. The full widths at half maximum (FWHMs) were 28 and 22 arcsec for the (0002) symmetric and (10$\bar{1}$2) asymmetric x-ray rocking curves of the AlN layer. The values are very small among heteroepitaxially grown AlN layers in other studies and reflect low dislocation density of the coherent AlN and uniform lattice constant (strain) through the AlN layer. To obtain accurate strain values of the AlN layer, accurate lattice constants of bulk AlN are needed. We also measured the lattice constants of high-quality bulk AlN grown by PVT method, resulting in a = 3.1113 Å and c = 4.9807 Å. The obtained lattice constants agree with the other report[21] within an error of < 0.01%. Note that impurity concentrations of the bulk AlN are less than 3×10^{19} cm^{-3},[21] effects of which on lattice constants (strain) are negligible.[22] From the lattice constants of our AlN layer and the bulk AlN, the in-plane ($\epsilon_{xx} = \epsilon_{yy}$) and out-of-plane ($\epsilon_{zz}$) strains of the coherent AlN were obtained to be −0.95 ± 0.02 and 0.514 ± 0.04%, respectively.

Phonon modes were characterized by a micro Raman system (T64000, HORIBA) with an Ar^+ laser probe (λ = 488.0 nm). The measurements were performed with the geometry of $z(x,x)\bar{z} + z(x,y)\bar{z}$ (backscattering). The spectra were collected using charge-coupled device camera cooled by liquid nitrogen. Raman spectra of the bulk AlN were also obtained as strain-free values of each peak. The Ar plasma line at 496.5 nm was used to calibrate the spectra. Peaks are fitted using Lorentzian function.

Raman scattering spectra of the coherent (highly strained) AlN and the bulk (strain-free) AlN are shown in Fig. 1. The Raman spectra from the E_2 (low), E_2 (high), and A_1 (LO) phonon modes are obtained. Raman scattering spectra of SiC substrate without an AlN epitaxial layer are also shown in Fig. 1. The E_2 (FTA) mode from SiC exists at 241 cm^{-1}, which does not largely superimpose the E_2 (low) mode of the coherent AlN. Around the E_2 (high) mode, there is no peak from the SiC substrate. Then, peak positions of the E_2 (low) and E_2 (high) mode in the coherent AlN can easily be determined with fitting curves, which are shown as solid lines in Figs. 1(a) and (b). On the other hand, the A_1 (LO) mode of the coherent AlN is partly hindered by the A_1 + E_1 (FLO) mode at 883 and 889 cm^{-1} and a weak peak at 905 cm^{-1} of SiC as can be seen in Fig. 1(c). To determine the peak position of the A_1 (LO) mode of the coherent AlN, curve fitting was performed with four Lorentzian peaks (one for AlN and three for SiC). The obtained fitting curve of the A_1 (LO) mode from the coherent AlN is also shown as a red solid line in Fig. 1(c).

The FWHMs of the Raman spectra are almost equal to those values of the bulk AlN, reflecting high crystalline quality of the coherent AlN. From the above fitting curves, the phonon frequencies of the E_2 (low), E_2 (high), and A_1 (LO) modes of the coherent AlN are determined to be 244.5, 672.1, and 899 cm^{-1}, respectively. For the bulk AlN, the phonon frequencies are obtained as well (247.8, 655.8, and 888 cm^{-1} for E_2 (low), E_2 (high), and A_1 (LO) modes, respectively) By comparing the spectra of the unstrained bulk AlN, the phonon frequencies of the E_2 (low), E_2 (high), and A_1 (LO) modes of the coherent AlN are found to shift in the values of −3.3, +16.3, and +11 cm^{-1}, respectively,

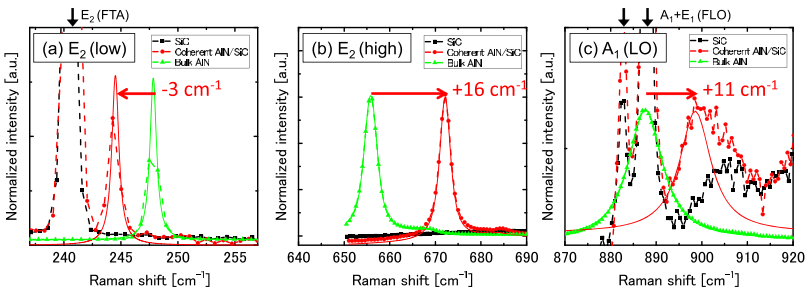

FIG. 1. Raman spectra of coherent AlN/SiC, bulk (unstrained) AlN, and SiC substrate. Raman shifts of the E_2 (low), E_2 (high) and A_1 (LO) modes are shown. Solid lines are fitting curves for each phonon mode of AlN by Lorentzian functions. Peaks from SiC substrate are indicated with arrows.

TABLE I. Frequency shifts of the E_2 (low), E_2 (high) and A_1 (LO) modes in AlN coherently grown on SiC. Reported PDPs of each phonon mode and expected frequency shifts using each PDP and strain values of the AlN coherently grown on SiC are also shown.

							Our experiments [cm^{-1}]		
							$\Delta\omega_{E_2(low)}$	$\Delta\omega_{E_2(high)}$	$\Delta\omega_{A_1(LO)}$
							−3.3	**16.3**	**11**
	Reported α, β [cm^{-1}]						Expected frequency shifts for AlN coherently grown on SiC [cm^{-1}]		
	E_2 (low)		E_2 (high)		A_1(LO)				
	α	β	α	β	α	β	$\Delta\omega_{E_2(low)}$	$\Delta\omega_{E_2(high)}$	$\Delta\omega_{A_1(LO)}$
ab initio calculation	149	−223	−881	−906	−739	−737[a]	−4.0	12.2	10.5
Experiments			−1008	−1083[b]				13.7	
			−1092	−965	−643	−1157[c]		16.0	6.4
			−1230	−940[d]				18.8	
			−1134	−1116	−960	−632[e]		16.0	15.2
	116	−224	−1210	−1015	−606	−1052[f]	−3.4	18.0	6.2
	108	−237	−1145	−1023	−576	−1079[g]	−3.3	16.7	5.5

[a]Ref. 8, *ab initio.*
[b]Ref. 9, mechanical bending (AlN on Si).
[c]Ref. 10, relaxed (AlN buffer layer for growth of AlN/GaN superlattices on SiC).
[d]Ref. 11, relaxed (AlN on sapphire or SiC).
[e]Ref. 12, ball-on-ring flexure (AlN on Si).
[f]Ref. 14, uniaxial pressure (high-quality AlN bulk).
[g]PDPs of Ref. 14 recalculated by using the elastic constants of Ref. 17.

which are listed in Table I. Note that the intensity of the A_1 (LO) mode from our coherent AlN is weak and there are several peaks from SiC substrates around the peak as discussed above, resulting that accurate determination of the the A_1 (LO) mode frequency is difficult. At least, the frequency shift of the A_1 (LO) mode is more than 10 cm^{-1}.

Phonon frequency shift $\Delta\omega$ is given by the following equation under equibiaxially strained ($\epsilon_{xx} = \epsilon_{yy}$) condition,

$$\Delta\omega = \alpha(\epsilon_{xx} + \epsilon_{yy}) + \beta\epsilon_{zz} = 2\alpha\epsilon_{xx} + \beta\epsilon_{zz}, \quad (1)$$

where α and β are the PDPs. The PDPs of each phonon mode have been reported theoretically and experimentally.[8–13] Frequency shifts derived from the reported PDPs and the strain values of the coherent AlN are listed in Table I. Methods used to obtain the reported PDPs are also shown in its footnote.

As can be seen, there are large discrepancies among the reported PDPs. For the PDPs of Refs. 9–12 (b–e in Table I), these disagreements partly originate from low crystalline quality of AlN because the AlN layers are heteroepitaxially grown and include high density of defects. On the other hand, the PDPs in Ref. 14 (f in Table I) are relatively reliable since they used high-quality bulk AlN. Moreover, they experimentally obtained the PDPs of the E_2 (low) mode for the first time and the expected frequency shift agrees well with our result. On the other hand, the E_2 (high) and A_1 (LO) modes exhibit 10 and 50% errors, respectively, which are large even if considering measurement errors of our results. For those phonon modes, the PDPs in Ref. 12 (e in Table I), obtained by ball-on-ring flexure for AlN on Si, give closer values for our results. To avoid inaccuracy originating from crystalline defects in AlN, we especially focus on the PDPs obtained through high-quality bulk AlN (f in Table I, Ref. 14) in the following discussion.

In the past study, we reported that shifts of free exciton transition energies in the coherent AlN is slightly different from the values derived from the (electronic band) deformation potentials and the elastic stiffness constants of AlN.[20] We conjectured that the difference came from inaccuracy of the elastic stiffness constants and the same thing may happen in the PDPs. Actually, in Ref. 14, the

PDPs are derived from following equation using the elastic stiffness constants,

$$\alpha = \tilde{\alpha}(C_{11} + C_{12}) + \tilde{\beta}C_{13},\ \beta = 2\tilde{\alpha}C_{13} + \tilde{\beta}C_{33}, \tag{2}$$

where $\tilde{\alpha}$ and $\tilde{\beta}$ are the phonon pressure coefficients (PPCs). Callsen et al. applied uniaxial pressure to bulk AlN and obtained pressure dependence of frequency shifts in each phonon mode, which corresponds to $\tilde{\beta}$.[14] To obtain PDPs, they used hydrostatic pressure dependence of frequency shifts in each phonon mode of bulk AlN, which corresponds to $2\tilde{\alpha} + \tilde{\beta}$, reported by Manjón, et al.[23] These PPCs are obtained from high-quality bulk AlN, leading to accurate values of the PPCs. However, accuracy of the PDPs clearly depends on accuracy of the elastic stiffness constants, which should be considered. In Ref. 14, they used the elastic stiffness constants reported by McNeil, et al.[24] Ishii et al. recently reported that the elastic stiffness constants reported by Kazan, et al.[17] well explained uniaxial pressure dependence of free exciton transition energies in bulk AlN.[25] In addition, shifts of free exciton energies in the coherent AlN are fairly explained by the Kazan's elastic stiffness constants.[20] Based on these facts, we recalculated the PDPs using the data in Refs. 14 and 23 and the elastic constants in Ref. 17, which are shown in Table I (g). Estimated frequency shifts from the PDPs are also listed.

Considering errors of the PDP values, the expected frequency shift of the E_2 (high) mode from the recalculated PDPs agrees well with the shift of the coherent AlN. Therefore, we strongly recommend the PDPs derived from Refs. 14, 17 and 23 for E_2 (high) mode ($\alpha = -1145\ \mathrm{cm}^{-1}$ and $\beta = -1023\ \mathrm{cm}^{-1}$) at the present time.

The A_1 (LO) mode still yields large error, which is likely due to weakness of the A_1 (LO) mode. In Ref. 23, only A_1 (LO) mode shows relatively large error in the hydrostatic pressure dependence (they mentioned that the weakness of the A_1 (LO) mode likely leads to inaccurate determination of the PPCs). In Ref. 14, A_1 (LO) mode is forbidden in the configuration (*a*-axis backscattering geometry). For the A_1 (LO) mode, the PDPs in Ref. 12 gives the value closer to our result. It should be pointed out that LO phonon plasmon coupling (LOPC) affects the peak position of A_1 (LO) phonon mode. The impurity concentrations of Si and O, which become donor in AlN, in the coherent AlN layer are 2×10^{16} and $2 \times 10^{17}\ \mathrm{cm}^{-3}$, respectively. Thus, the carrier concentration is much low and the peak position of the A_1 (LO) mode is not affected by the LOPC.

Among Raman active phonon modes of *c*-oriented AlN layers in a backscattering geometry, the E_2 (high) mode is widely used to determine strain in an AlN layer because of its strong interaction to photons and high sensitivity to strain. To obtain strain values only from a frequency shift of the E_2 (high) mode, the following equation is needed,

$$\epsilon_{xx} = -\frac{C_{33}}{2C_{13}}\epsilon_{zz}, \tag{3}$$

where C_{ij} are the elastic stiffness constants. Then, Eq. (1) only depends on ϵ_{zz},

$$\Delta\omega = \left(-\frac{C_{33}}{C_{13}}\alpha + \beta\right)\epsilon_{zz}. \tag{4}$$

As mentioned in the introduction, the reported elastic stiffness constants are different from report to report. Even when using the recently reported values in Ref. 17 with the ϵ_{zz} of the coherent AlN/SiC, the estimated frequency shift is $+19.6\ \mathrm{cm}^{-1}$, which largely differs from our result ($+16.3\ \mathrm{cm}^{-1}$). Though accuracy of the PDPs and the elastic stiffness constants needs to be discussed, the coefficient of Eq. (4) can experimentally be obtained with values of $\Delta\omega_{E_2(high)}$ and ϵ_{zz}. Then, we obtained $\Delta\omega_{E_2(high)}$-ϵ_{zz} relationship only from our data as following,

$$\Delta\omega_{E_2(high)} = (3.2 \times 10^3\ \mathrm{cm}^{-1}) \times \epsilon_{zz}. \tag{5}$$

In conclusion, the phonon frequencies of the AlN coherently grown on SiC and the bulk AlN were measured by Raman scattering. The FWHMs of the Raman peaks from the coherent AlN were similar to those of the bulk AlN, reflecting high crystalline quality of the coherent AlN. The large phonon frequency shifts due to the large compressive strain were observed. The frequency shifts were estimated by using the reported PDPs and the strains of the coherent AlN. By combining the reliable data sets of the PPCs in Refs. 14 and 23 and the elastic stiffness constants in Ref. 17, the PDPs of the E_2 (high) mode were obtained, which values gave the results consistent with our experimental data.

ACKNOWLEDGMENTS

This work was supported by a Grant-in-Aid for JSPS Fellows (26.7117).

[1] J. Tajima, C. Echizen, R. Togashi, H. Murakami, Y. Kumagai, K. Takada, and A. Koukitu, Jpn. J. Appl. Phys. **50**, 055501 (2011).
[2] H. Siegle, A. Hoffmann, L. Eckey, C. Thomsen, J. Christen, F. Bertram, D. Schmidt, D. Rudloff, and K. Hiramatsu, Appl. Phys. Lett. **71**, 2490 (1997).
[3] Y. Wang, N. Yu, C. Wang, and K. Lau, Adv. Mat. Res. **396**, 372 (2012).
[4] S. L. Selvaraj, A. Watanabe, and T. Egawa, Appl. Phys. Lett. **98**, 252105 (2011).
[5] H. Harima, J. Phys.: Condens. Matter **14**, R967 (2002).
[6] G. Callsen, J. S. Reparaz, M. R. Wagner, R. Kirste, C. Nenstiel, A. Hoffmann, and M. R. Phillips, Appl. Phys. Lett. **98**, 061906 (2011).
[7] V. Darakchieva, T. Paskova, M. Schubert, H. Arwin, P. P. Paskov, B. Monemar, D. Hommel, M. Heuken, J. Off, F. Scholz, B. A. Haskell, P. T. Fini, J. S. Speck, and S. Nakamura, Phys. Rev. B **75**, 195217 (2007).
[8] J. M. Wagner and F. Bechstedt, Phys. Rev. B **66**, 115202 (2002).
[9] A. Sarua, M. Kuball, and J. E. Van Nostrand, Appl. Phys. Lett. **81**, 1426 (2002).
[10] J. Gleize, M. A. Renucci, J. Frandon, E. Bellet-Amalric, and B. Daudin, J. Appl. Phys. **93**, 2065 (2003).
[11] S. Yang, R. Miyagawa, H. Miyake, K. Hiramatsu, and H. Harima, Appl. Phys. Express **4**, 031001 (2011).
[12] W. Zhu, A. Leto, K. Y. Hashimoto, and G. Pezzotti, J. Appl. Phys. **112**, 103526 (2012).
[13] V. Darakchieva, P. P. Paskov, T. Paskova, J. Birch, S. Tungasmita, and B. Monemar, Appl. Phys. Lett. **80**, 2302 (2002).
[14] G. Callsen, M. R. Wagner, J. S. Reparaz, F. Nippert, T. Kure, S. Kalinowski, A. Hoffmann, M. J. Ford, M. R. Phillips, R. F. Dalmau, R. Schlesser, R. Collazo, and Z. Sitar, Phys. Rev. B **90**, 205206 (2014).
[15] I. Vurgaftman and J. R. Meyer, J. Appl. Phys. **94**, 3675 (2003).
[16] K. Kim, W. R. L. Lambrecht, and B. Segall, Phys. Rev. B **53**, 16310 (1996).
[17] M. Kazan, E. Moussaed, R. Nader, and P. Masri, Phys. Status Solidi C **4**, 204 (2007).
[18] H. Okumura, T. Kimoto, and J. Suda, Appl. Phys. Express **4**, 025502 (2011).
[19] H. Okumura, T. Kimoto, and J. Suda, Appl. Phys. Express **5**, 105502 (2012).
[20] M. Kaneko, H. Okumura, R. Ishii, M. Funato, Y. Kawakami, T. Kimoto, and J. Suda, Appl. Phys. Express **6**, 062604 (2013).
[21] Y. Kumagai, Y. Kubota, T. Nagashima, T. Kinoshita, R. Dalmau, R. Schlesser, B. Moody, J. Xie, H. Murakami, A. Koukitu, and Z. Sitar, Appl. Phys. Express **5**, 055504 (2012).
[22] M. Leszczynski, H. Teisseyre, T. Suski, I. Grzegory, M. Bockowski, J. Jun, S. Porowski, K. Pakula, J. M. Baranowski, C. T. Foxon, and T. S. Cheng, Appl. Phys. Lett. **69**, 73 (1996).
[23] F. J. Manjón, D. Errandonea, A. H. Romero, N. Garro, J. Serrano, and M. Kuball, Phys. Rev. B **77**, 205204 (2008).
[24] L. E. McNeil, M. Grimsditch, and R. H. French, J. Am. Ceram. Soc. **76**, 1132 (1993).
[25] R. Ishii, A. Kaneta, M. Funato, and Y. Kawakami, Phys. Rev. B **87**, 235201 (2013).